ON THE DYNAMICS OF THE SOLAR CORONA: THE NUMERICS BEHIND A SELF-CONSISTENT 3D MHD MODEL

J. Kleimann[1], **H. Fichtner**[1], **A. Kopp**[1], **K. Germaschewski**[2], **and R. Grauer**[2]

[1]Institut für Theoretische Physik IV, Ruhr-Universität Bochum, 44780 Bochum, Germany
[2]Institut für Theoretische Physik I, Ruhr-Universität Bochum, 44780 Bochum, Germany

ABSTRACT

Space missions like SOHO have renewed the interest in the physics of the solar corona. This complex system is not yet fully understood due to lack of sufficiently detailed observations, and also because realistic models should cover processes occurring on various spatial scales, while being both multidimensional and time-dependent. Significant progress w.r.t. their numerical realization was achieved recently with the *Central Weighted Essentially Non-Oscillatory* scheme. A 3rd order CWENO scheme efficiently capturing strong gradients forms the basis of our new code. After describing the algorithm and its implementation, we present test results as well as comparisons with preexisting codes.

Key words: solar wind; MHD; numerical simulation.

1. CONCEPT OF NON-OSCILLATORY SCHEMES

Consider the (frequent) case of a quantity $u = u(x,t)$ whose evolution is governed by a convection-diffusion equation

$$\partial_t \, u + \partial_x f(u) = Q(u, \partial_x u) \ , \qquad (1)$$

with vector-valued functions f (nonlinear convection flux) and Q (source term). If $Q = 0$, u is a *conserved quantity* and (1) is called a *hyperbolic conservation law.*

Aim: find (approximate) solutions to (1) on a spatial grid of finite extension and spacing.

1.1. Non-oscillatory Reconstruction

Steps to discretize (1) (for $Q = 0$) on a grid of cell size Δx:

- Let
$$\bar{u}_j^n := \frac{1}{\Delta x} \int_{x_{j-1/2}}^{x_{j+1/2}} u(x, t^n) \; dx \qquad (2)$$
be the cell average of u at time $t = t^n := n \; \Delta t$ and location $x = x_j := j \; \Delta x$. Sampling (1) at the cells $I_{j+1/2} := [x_j, x_{j+1}]$ and integrating from t^n to t^{n+1} yields
$$\begin{aligned} \bar{u}_{j+1/2}^{n+1} &= \bar{u}_{j+1/2}^{n} - (\Delta x)^{-1} \times \\ &\times \int_{t^n}^{t^{n+1}} \left[f(u(x_{j+1}, \tau)) - f(u(x_j, \tau)) \right] d\tau \end{aligned} \qquad (3)$$
as an *exact* equation for the cell average's time evolution.

- Define polynomials $P_j(x)$ which approximate the solution u in each cell $I_j \;\Rightarrow\;$ cell average $\bar{u}(x)$ at time t^n and position $x_{j+1/2}$ given by
$$\begin{aligned} \bar{u}_{j+1/2}^{n} &= \frac{1}{\Delta x} \left(\int_{x_j}^{x_{j+1/2}} P_j(x) \; dx \; + \right. \\ &+ \left. \int_{x_{j+1/2}}^{x_{j+1}} P_{j+1}(x) \; dx \right) \; . \end{aligned} \qquad (4)$$

How should the P_j be chosen?

⋄ <u>simple choice:</u>

$$P_j(x) = \bar{u}_j \quad \text{(piecewise constant) and}$$
$$\int_{t^n}^{t^{n+1}} f[u(t)] \; dt \approx f(\bar{u}^n) \; \Delta t \quad \text{first-order quadrature}$$

$$\Longrightarrow \; \bar{u}_{j+1/2}^{n+1} = \frac{\bar{u}_{j+1}^n + \bar{u}_j^n}{2} - \frac{\Delta t}{\Delta x} \left[f(\bar{u}_{j+1}^n) - f(\bar{u}_j^n) \right] \qquad (5)$$

(staggered Lax-Friedrichs scheme, not good due to strong numerical dissipation $\propto (\Delta x)^2 / \Delta t$)

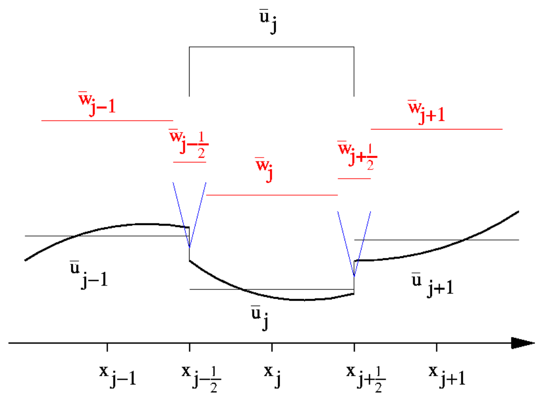

Figure 1. CWENO differencing. The representation of $u(x)$ using cell polynomials causes discontinuities at the cell boundaries which propagate within the Riemann fans. Both grids, smooth and non-smooth, are integrated in time and then projected back onto the uniform grid.

◇ CWENO (Kurganov & Levy [2000])

This scheme uses for P_j a convex sum of two linear polynomials $P_{\mathrm{L},j}$ and $P_{\mathrm{R},j}$, and one parabola $P_{\mathrm{C},j}$ centered at x_j:

$$P_j(x) = \sum_{\alpha \in \{\mathrm{R,C,L}\}} w_\alpha P_{\alpha,j}(x) \tag{6}$$

with $\sum_\alpha w_\alpha = 1$. $P_{\mathrm{C},j}$ is defined by

$$\sum_{\alpha \in \{\mathrm{R,C,L}\}} c_\alpha P_{\alpha,j}(x) = P_{\mathrm{exact},j} \ , \tag{7}$$

such that $P_{\mathrm{R},j}(x_j) = \bar{u}_j$, $P_{\mathrm{R},j}(x_{j+1}) = \bar{u}_{j+1}$ and analogously for $P_{\mathrm{L},j}$ and $P_{\mathrm{exact},j}$, i.e., they reproduce the cell averages, thus ensuring flux conservation.

For a central scheme, the c_α are chosen symmetrically, e.g., $c_{\mathrm{L}} = c_{\mathrm{R}} = 1/4$, $c_{\mathrm{C}} = 1/2$, which can be shown to guarantee third-order accuracy.

Problem: Strong gradients tend to cause spurious oscillations.

Solution: check the difference $(\bar{u}_j^n - \bar{u}_{j\pm1}^n)$ to neighboring cells and adjust the weights w_α such that the side which varies least provides the largest contribution to the construction of P_j, while in smooth regions all components contribute equally.

1.2. Time Stepping

The polynomial reconstruction of u is smooth within each cell but discontinuous at the boundaries between adjacent cells.

Integration procedure:

- propagation speed $v_{\mathrm{shock},j}$ bounded by $a_j \Rightarrow$ shock emanating from $x = x_{j+1/2}$ confined by $\|x_{\mathrm{shock}}(t) - x_{j+1/2}\| \leq \|a_j(t - t^n)\|$ ("Riemann fan", wedge-shaped lines in Fig. 1).
- Integrating smooth and non-smooth region independently in time gives new averages $\bar{w}_j$ and $\bar{w}_{j+1/2}$ at time $t = t^{n+1}$.
- Projection of the $\bar{w}$'s back onto the original, uniform grid gives new values $\bar{u}^{n+1}$.
- Take limit $\Delta t \to 0$ to get a semi-discrete, third-order scheme and employ, e.g., 3rd order Runge-Kutta time stepping.

1.3. Resulting advantages of CWENO

- extension 1D → 3D is simple (dimension by dimension approach)
- built-in flux conservation
- does not require (approximate) Riemann solver
- avoids oscillations near huge gradients, while maintaining third-order precision in smooth regions

2. NUMERICAL TESTS

The evolution of a perfectly conducting fluid, characterized by

density ρ,	magnetic field $\mathbf{B}$,
velocity $\mathbf{v}$,	current density $\mathbf{j}$ and
gas pressure p,	

and subjected to gravity $\mathbf{g}$ is known to be governed by the following set of (dimensionless) MHD equations:

$$\begin{aligned}
\partial_t \rho &= -\nabla \cdot (\rho\ \mathbf{v}) && (8)\\
\partial_t(\rho\ \mathbf{v}) &= -\nabla \cdot \left(\rho\ \mathbf{vv} + (p + B^2/2)\underline{\mathbf{1}} - \mathbf{BB}\right) && (9)\\
&+\ \rho\ \mathbf{g} && (10)\\
\partial_t \mathbf{B} &= -\nabla \cdot (\mathbf{v}\ \mathbf{B} - \mathbf{B}\ \mathbf{v}) && (11)\\
\partial_t p &= -\nabla \cdot (p\ \mathbf{v}) - (\gamma - 1)\ p\ (\nabla \cdot \mathbf{v}) && (12)\\
p &= \rho\ T \quad \text{(ideal gas eq. of state).} && (13)
\end{aligned}$$

Various special cases have been used to detect code 'bugs':

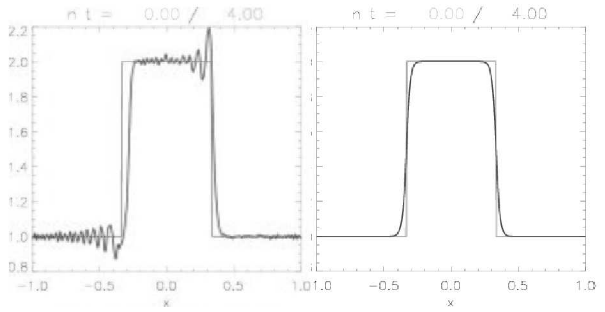

Figure 2. Advection test with periodic boundaries on a grid of 512 cells. Right: CWENO run. Left: comparison run using a standard leapfrog scheme, showing both initial profile and profile after one domain pass.

2.1. Linear Advection

In the absence of any acting force densities on the right hand side of the momentum equation (9), the one-dimensional version of (8) and (9) reads

$$\begin{aligned} \partial_t \rho + \partial_x (\rho\ v) &= 0 \qquad (14) \\ \rho\,(\partial_t v + v\ \partial_x v) &= 0\ , \qquad (15) \end{aligned}$$

with initial conditions

$$\begin{aligned} \rho(x,0) &= \rho_0(x) \\ v(x,0) &= v_0 \end{aligned} \qquad (16)$$

for $\rho = \rho(x,t)$ and $v = v(x,t)$. The known analytic solution is

$$\begin{aligned} \rho(x,t) &= \rho_0(x - v_0 t) \\ v(x,t) &= v_0 \end{aligned} \qquad (17)$$

and shows that the density profile is transported with a constant flow velocity v_0 and maintains its initial shape.
$\Rightarrow$ *All* deviations *must* be numerical artifacts.

The traditional leapfrog scheme (see Fig. 2, left) tends to produce spurious oscillations at the edges of the profile, whereas CWENO is able to effectively suppress these artifacts (Fig. 2.1 right).

2.2. Magnetized Shock Tube

Setting: two separate domains [1], [2]; initially

$$\mathbf{U}(x) = \begin{cases} \mathbf{U}_1 & \text{if} \quad x \in [1] \\ \mathbf{U}_2 & \text{if} \quad x \in [2] \end{cases}$$

- removal of membrane ($\Rightarrow$ free expansion) gives rise to traveling discontinuities (*shock fronts*).
- first proposed as a test by Sod [1978] using $\mathbf{U} = [\rho,\ P]$; extension to $B \neq 0$ by Brio & Wu [1987]

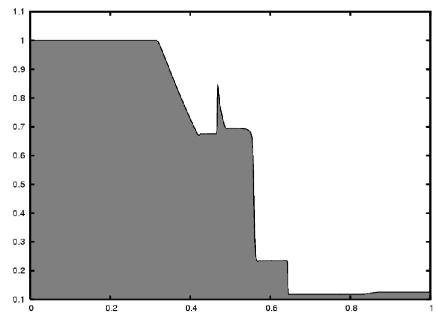

Figure 3. Density profile at $t = 0.1$. Location and slopes can be used to check for correct handling of strong gradients.

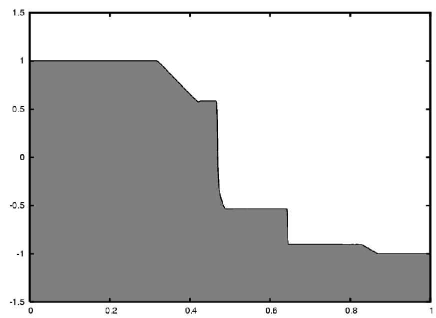

Figure 4. Corresponding profile of the transverse magnetic field along the tube axis.

The shock tube problem serves to check the code's ability to handle strong discontinuities and to correctly reproduce the Rankine-Hugoniot jump conditions.

2.3. The Rayleigh-Taylor Instability

This test setting consists of a fluid which is stratified with respect to gravity such that one homogeneous domain of high density is placed above a less denser one. This unstable configuration should give rise to the *Rayleigh-Taylor Instability* as soon as a perturbation of the horizontal interface occurs, and this can indeed be observed nicely in the sequence below.

3. ADAPTIVE MESH REFINEMENT

Fact : High spatial resolution wanted (and needed!)

Problem : limited resources (memory and CPU time)

$\Rightarrow$ **Solution :** increase resolution only where needed (e.g., at loci of strong gradients, etc.)

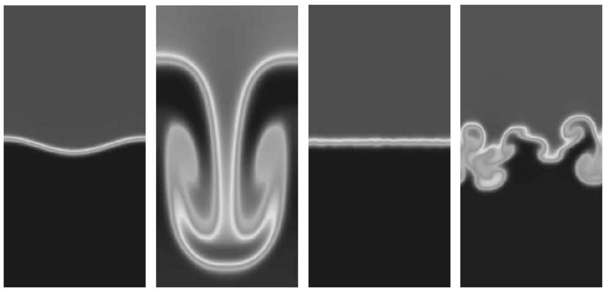

Figure 5. Two cases of Rayleigh-Taylor instability arising from a cosine (left) and a random perturbation, respectively. Shading codes fluid density (using a non-monotonous color table).

4. APPLICATION: SOLAR WIND MODELING

Application of our code to the dynamics of the *solar wind* is discussed during the oral presentation *On the dynamics of the solar corona: first results obtained with a new 3D MHD model* by Kleimann et al., this conference.

5. CONCLUSIONS AND OUTLOOK

- Successful implementation and extensive testing of a flux-conserving, shock-capturing, 3rd-order semi-discrete scheme
- combination with mesh refinement techniques allows for high effective resolutions as needed for full MHD solar wind modeling
- next step: implementation of *divergence cleaning routines* to numerically ensure $\nabla \cdot \mathbf{B} = 0$ throughout the simulation

ACKNOWLEDGMENTS

Financial support by the *Wernher von Braun-Foundation* is gratefully acknowledged.

REFERENCES

Brio & Wu [1987] *J. Comp. Phys.* **75**, 400.

Kurganov, A. & Levy, D. [2000] *SIAM J. Sci. Comput.* **22/4**, 1461.

Sod, G. [1978] *J. Comp. Phys.* **27**, 1.